JACS
JOURNAL OF THE AMERICAN CHEMICAL SOCIETY

COMMUNICATION

pubs.acs.org/JACS

Colloidal Iron Pyrite (FeS_2) Nanocrystal Inks for Thin-Film Photovoltaics

James Puthussery, Sean Seefeld, Nicholas Berry, Markelle Gibbs, and Matt Law*

Department of Chemistry and Department of Chemical Engineering and Materials Science, University of California, Irvine, California 92697, United States

Supporting Information

ABSTRACT: Iron pyrite (FeS_2) is a promising earth-abundant semiconductor for thin-film solar cells. In this work, phase-pure, single-crystalline, and well-dispersed colloidal FeS_2 nanocrystals (NCs) were synthesized in high yield by a simple hot-injection route in octadecylamine and then were subjected to partial ligand exchange with octadecylxanthate to yield stable pyrite NC inks. Polycrystalline pyrite thin films were fabricated by sintering layers of these NCs at 500−600 °C under a sulfur atmosphere.

Pyrite iron persulfide (β-FeS_2, fool's gold) is an underresearched semiconductor that is extremely promising for use as the active layer in solar photovoltaic and photoelectrochemical cells. Pyrite has a suitable band gap (E_g = 0.95 eV), strong light absorption ($\alpha > 10^5$ cm^{-1} for $h\nu > 1.3$ eV),[1] an adequate minority carrier diffusion length (100−1000 nm),[2,3] and essentially infinite elemental abundance. In principle, all of U.S. primary power demand (~3.5 TW) could be met with 10% of the pyrite that is disposed annually as mining waste in six U.S. states alone (assuming 10% cell efficiency and a conservative 5 μm thick pyrite active layer).[4] Pyrite photoelectrochemical and Schottky solar cells were first demonstrated by Tributsch in 1984.[5] Pyrite devices show high quantum efficiencies (often >90%) and photocurrents (>40 mA cm^{-2}) but small photovoltages (typically <200 mV, ~20% of the band gap).[6−10] The low photovoltage is attributed to sulfur vacancies in the bulk and at the surface that generate electronic states within the band gap.[11] Enhancing the photovoltage and efficiency of pyrite cells requires basic research on the growth, surface passivation, and structural and electronic characterization of pyrite films.[12]

Pyrite nanocrystals (NCs) are particularly appealing because of the prospect of fabricating inexpensive, large-area photovoltaics by the roll-to-roll deposition of NC solar ink or paint on flexible substrates. NC-based photovoltaics processed from solution may offer excellent manufacturing scalability at very low cost relative to conventional single-crystal and thin-film approaches. Recently, photovoltaics made from sintered layers of solution-deposited NCs have received considerable attention, and photovoltaic devices based on systems such as CdTe/CdSe,[13] $CuInSe_2$ and its related compounds,[14−16] and Cu_2ZnSnS_4[17−19] have been demonstrated. Pyrite NCs were first grown over a decade ago,[20] and more recently, syntheses of large pyrite aggregates[21] and clusters of small pyrite NCs[22] have been described. Here we present an approach for making high-quality pyrite NC thin films from stable colloidal dispersions of single-crystalline, phase-pure pyrite NCs. Sintering the NC films in

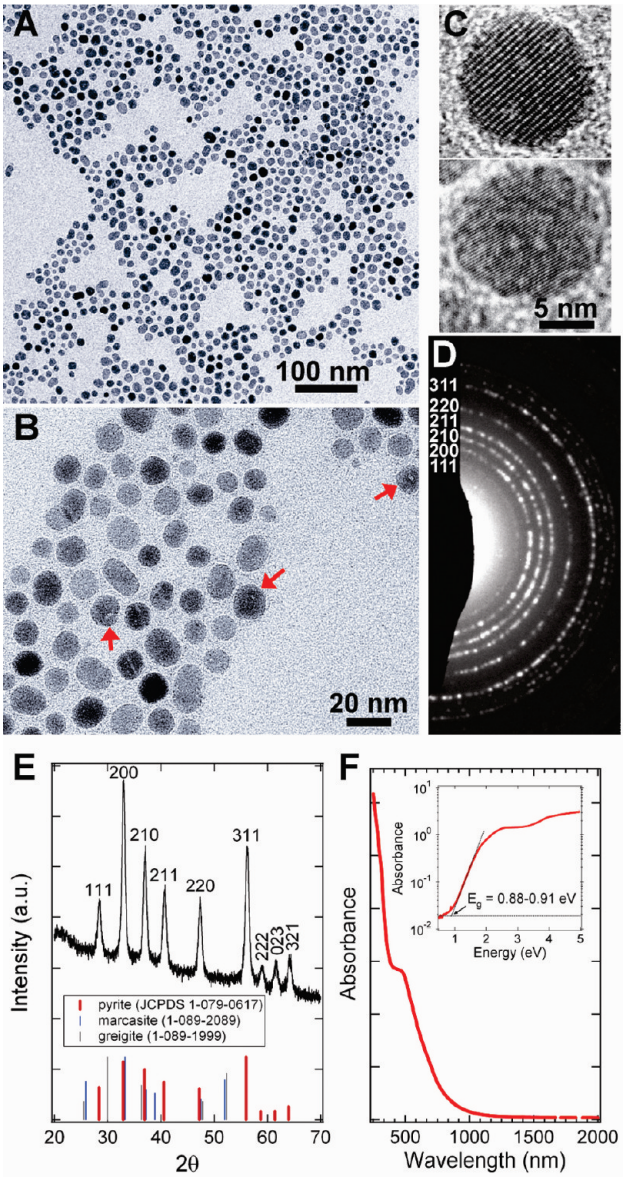

Figure 1. TEM, ED, XRD, and UV−vis spectroscopic characterization of the colloidal pyrite nanocrystals.

Received: October 26, 2010
Published: December 22, 2010

   dx.doi.org/10.1021/ja1096368 | J. Am. Chem. Soc. 2011, 133, 716–719

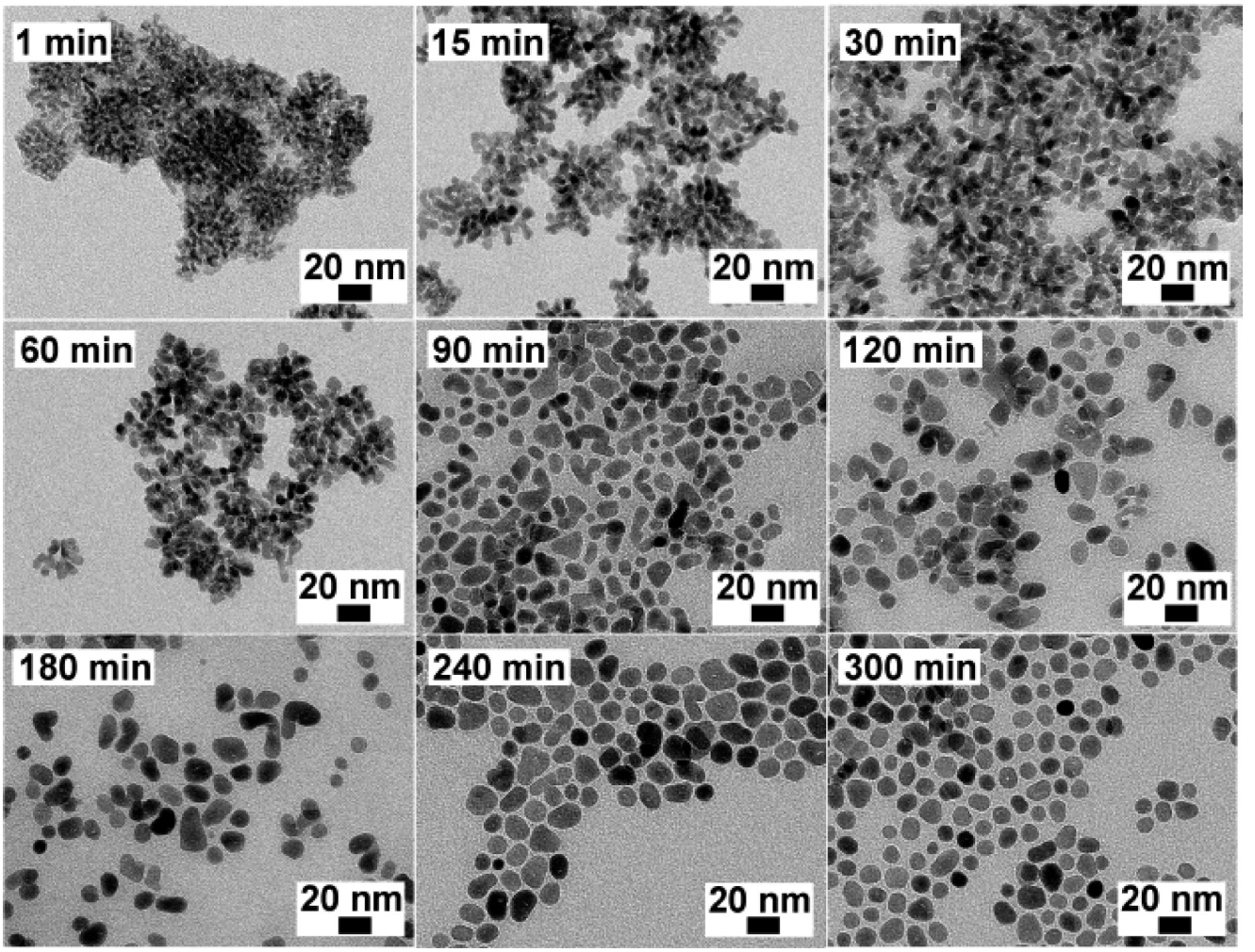

Figure 2. Time series of TEM images of the pyrite NC reaction.

sulfur at moderate temperatures (500−600 °C) produces large-grain polycrystalline pyrite films that hold promise for use as the active layer of solar cells.

We prepared colloidal pyrite NCs by injecting a solution of sulfur dissolved in diphenyl ether into a solution of $FeCl_2$ in octadecylamine at 220 °C and stirring for several hours, after which the NCs were purified using standard precipitation and suspension techniques (see the Supporting Information for details). Figure 1 presents basic structural characterization data for the purified colloids. The NCs are a mixture of oblate and spheroidal single crystals with diameters of 5−20 nm. Many of the NCs have a doughnutlike appearance, with depressions or holes in their centers (red arrows in Figure 1B; also see Figure S1 in the Supporting Information). Lattice-resolved transmission electron microscopy (TEM) images (Figure 1C) indicate that the NCs possess crystalline surfaces with no sign of an oxide coating or amorphous overlayer. Electron diffraction (ED) and X-ray diffraction (XRD) show that the NCs are single-phase pyrite without detectable marcasite, greigite, pyrrhotite, or other impurities (Figure 1D,E). IR spectra of dip-coated NC films show strong pyrite modes at 403, 348, and 293 cm^{-1}, providing further evidence for the phase purity of the product (Figure S2).[23] UV−vis absorption spectra of NC samples in chloroform indicate an absorption onset of ∼0.9 eV and a slow, monotonic absorption rise with a shoulder at ∼2.85 eV (Figure 1F).

It was difficult to accurately determine the band gap of the NCs because of the gradual absorption rise as well as the presence of light scattering and, possibly, an Urbach tail of defect states. On the basis of a semilog plot of the data (Figure 1F inset), we estimated the band gap of the NCs to be 0.88−0.91 eV, but in view of the complications mentioned above, this range of values is probably an underestimate. Rigorous measurements of the absorption coefficient of pyrite films made from these NCs are ongoing.

TEM images of aliquots removed at different stages of the reaction reveal that the doughnuts form via the fusion of several smaller, irregularly shaped pyrite NCs, which themselves gradually nucleate from an amorphous iron sulfide matrix present in the solution at lower temperatures (Figure 2). The amorphous material is consumed over several hours at the reaction temperature to yield the pyrite NC product. Pyrite was the only crystalline phase detected at any stage of the reaction.

Although the NCs form in high yield (>90%), a large fraction aggregate and become insoluble during purification, suggesting that octadecylamine is an unsuitable ligand for preparing stable pyrite NC inks. We found that partial ligand exchange with octadecylxanthate ($C_{18}H_{37}OCS_2^-$) reverses this precipitation and gives stable colloidal dispersions in chloroform (Figure S3). Xanthates are commonly used in the froth flotation of pyrite-bearing ores in commercial mining operations.[24]

dx.doi.org/10.1021/ja1096368 |*J. Am. Chem. Soc.* 2011, 133, 716–719

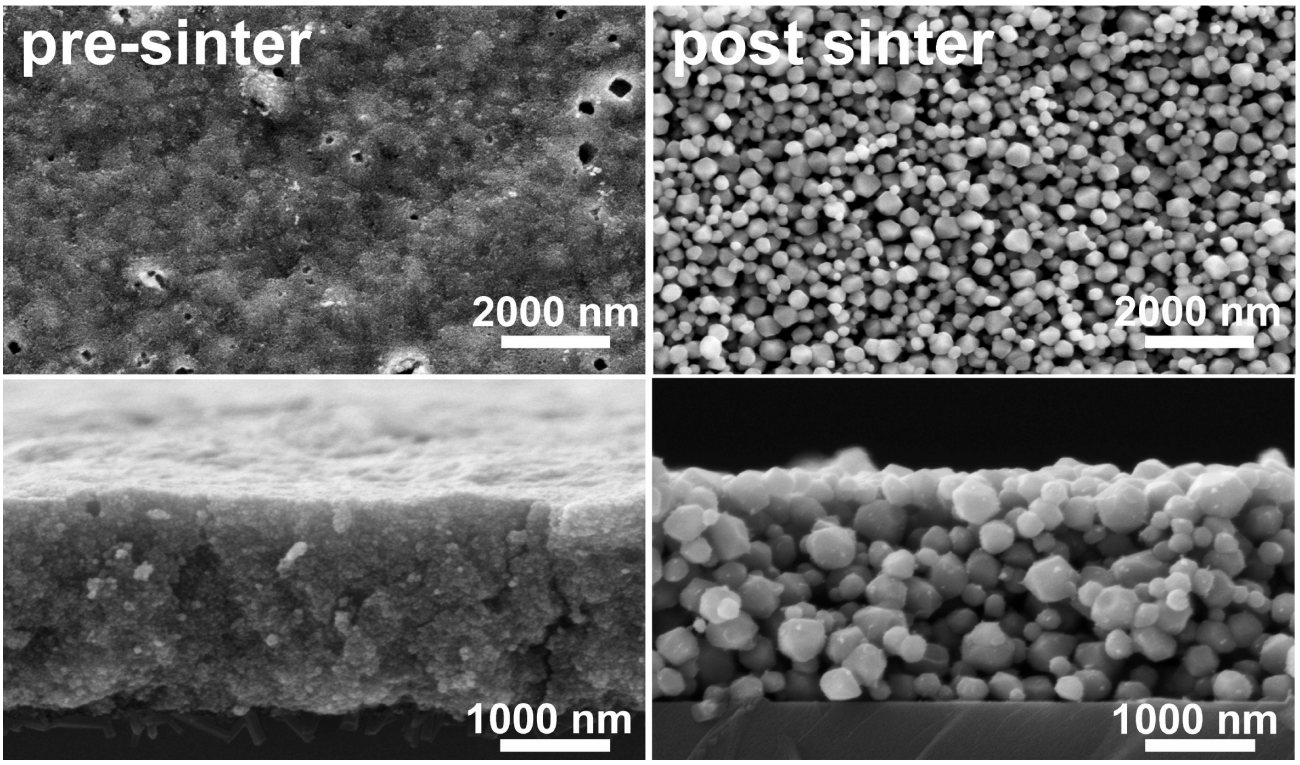

Figure 3. Top- and side-view SEM images of a pyrite NC film on a glass substrate before and after sintering at 540 °C in sulfur vapor.

Thin films of pyrite NCs were deposited on various substrates (glass, quartz, and silicon) using layer-by-layer dip-coating from chloroform solution (see the Supporting Information). A dipping cycle consisted of immersing the substrates in the pyrite NC ink, allowing them to dry, and then dipping them in 1 M hydrazine in acetonitrile, which served to insolubilize the NCs by removing a large fraction of the long-chain ligands from their surfaces (as verified by FTIR). Films were made using 25−100 dipping cycles. To produce larger-grain polycrystalline pyrite films suitable for solar cells, the NC layers were sintered in sulfur vapor at 500−600 °C in sealed quartz ampules. The purpose of sintering the NC films was to increase the average grain size (and thus the carrier diffusion length), reduce possible sulfur deficiency, remove carbon, and densify the films. Figure 3 shows plane-view and cross-section scanning electron microscope (SEM) images of a 2000 nm thick pyrite NC film on a glass substrate before and after sintering at 540 °C for 4 h. Under these conditions, sintering resulted in significant grain growth (average apparent grain size of ∼300 nm based on the SEM images and XRD), roughening of the film surface, and the formation of voids. In general, the microstructure obtained after sulfurization is a strong function of the film thickness, sintering temperature and time, ramping rates, sulfur partial pressure, and substrate. Higher temperatures yielded larger crystallites (up to ∼1 μm) and usually poorer intergrain connectivity and substrate coverage. Higher sulfur partial pressures also favored larger grains but gave better grain connectivity and fewer voids. Pyrite was the only phase detected by far-IR spectroscopy and XRD after sintering at temperatures below 650 °C (Figures S3 and S4, respectively; pyrrhotite began to form above this point). Optimization of the film microstructure as well as detailed electrical and optical measurements are underway.

When stored in a nitrogen-filled glovebox, the pyrite NC solutions and unsintered NC films were stable for at least 9 months with no apparent change in their XRD patterns or absorption spectra. On the other hand, chloroform solutions of amine/ammonium-capped NCs without xanthate showed complete decomposition within weeks of storage in air in the dark, leaving a yellow precipitate and clear supernatant. We have not yet carried out air stability tests for xanthate-capped NC solutions. Detailed characterization of the NC decomposition products and the impact of the capping ligand on degradation needs further extensive studies.

Pyrite NC thin films were observed to change color from gold to black after a few weeks in air. XRD of NC films exposed to air for 3 months showed the presence of hydrated iron sulfates and FeS species (Figure S5). However, once sintered, the polycrystalline pyrite films were stable for at least 1 month in air without discoloration or the appearance of new phases in XRD patterns. It is not surprising that large-grain pyrite films are more robust in air than films composed of high-surface-area nanocrystals. Since solid-state pyrite solar cells will likely utilize dense, large-grain thin films, oxidation should be manageable using common photovoltaic encapsulants and barrier coatings.

We have described the synthesis of phase-pure and stable colloidal pyrite NC inks via a simple hot-injection route and shown that polycrystalline pyrite films can be produced on various substrates by sintering films of these NCs in sulfur vapor. This approach is promising for low-cost, large-area, solution-based processing of pyrite thin films for photovoltaics.

■ ASSOCIATED CONTENT

Supporting Information. Synthetic details, additional TEM images, and FTIR and XRD characterization of the NCs

and polycrystalline thin films. This material is available free of charge via the Internet at http://pubs.acs.org.

AUTHOR INFORMATION

Corresponding Author
matt.law@uci.edu

ACKNOWLEDGMENT

We thank the NSF SOLAR Program (Award CHE-1035218) and the UCI School of Physical Sciences Center for Solar Energy for support of this work and acknowledge the provision of instrumentation in the Carl Zeiss Center of Excellence at UCI by Carl Zeiss SMT.

REFERENCES

(1) Altermatt, P. P.; Kiesewetter, T.; Ellmer, K.; Tributsch, H. *Sol. Energy Mater. Sol. Cells* **2002,** *71*, 181.
(2) Ennaoui, A.; Tributsch, H. *Sol. Energy Mater.* **1986,** *14*, 461.
(3) Smestad, G.; Ennaoui, A.; Fiechter, S.; Tributsch, H.; Hofmann, W. K.; Birkholz, M.; Kautek, W. *Sol. Energy Mater. Sol. Cells* **1990,** *20*, 149.
(4) Tao, D.; Abdelkhalck, M.; Chen, S.; Parekh, B. K.; Hepworth, M. T. *Environ. Issues Manage. Waste Energy Miner. Prod., Proc. Int. Conf. 6th* **2000,** 347.
(5) Ennaoui, A.; Tributsch, H. *Sol. Cells* **1984,** *13*, 197.
(6) Ennaoui, A.; Fiechter, S.; Smestad, G.; Tributsch, H. In *World Renewable Energy Congress: Energy and the Environment*; Sayigh, A. A. M., Ed.; Pergamon Press: Oxford, U.K., 1990; p 458.
(7) Ennaoui, A.; Fiechter, S.; Jaegermann, W.; Tributsch, H. *J. Electrochem. Soc.* **1986,** *133*, 97.
(8) Antonuccia, V.; Arico', A. S.; Giordano, N.; Antonucci, P. L.; Russo, U.; Cocke, D. L.; Crea, F. *Sol. Cells* **1991,** *31*, 119.
(9) Ennaoui, A.; Fiechter, S.; Tributsch, H.; Giersig, M.; Vogel, R.; Weller, H. *J. Electrochem. Soc.* **1992,** *139*, 2514.
(10) Blenk, O. Ph.D. Thesis, University of Konstanz, Konstanz, Germany, 1995 (in German).
(11) Birkholz, M.; Fiechter, S.; Hartmann, A.; Tributsch, H. *Phys. Rev. B* **1991,** *43*, 11926.
(12) Ennaoui, A.; Fiechter, S.; Pettenkofer, C.; Alonso-Vante, N.; Buker, K.; Bronold, M.; Hopfner, C.; Tributsch, H. *Sol. Energy Mater. Sol. Cells* **1993,** *29*, 289.
(13) Gur, I.; Fromer, N. A.; Geier, M. L.; Alivisatos, A. P. *Science* **2005,** *310*, 462.
(14) Guo, Q.; Kim, S. J.; Kar, M.; Shafarman, W. N.; Birkmire, R. W.; Stach, E. A.; Agrawal, R.; Hillhouse, H. W. *Nano Lett.* **2008,** *8*, 2982.
(15) Guo, Q.; Ford, G. M.; Hillhouse, H. W.; Agrawal, R. *Nano Lett.* **2009,** *9*, 3060.
(16) Panthani, M. G.; Akhavan, V.; Goodfellow, B.; Schmidtke, J. P.; Dunn, L.; Dodabalapur, A.; Barbara, P. F.; Korgel, B. A. *J. Am. Chem. Soc.* **2008,** *130*, 16770.
(17) Guo, Q.; Hillhouse, H. W.; Agrawal, R. *J. Am. Chem. Soc.* **2009,** *131*, 11672.
(18) Steinhagen, C.; Panthani, M. G.; Akhavan, V.; Goodfellow, B.; Koo, B.; Korgel, B. A. *J. Am. Chem. Soc.* **2009,** *131*, 12554.
(19) Riha, S. C.; Parkinson, B. A.; Prieto, A. L. *J. Am. Chem. Soc.* **2009,** *131*, 12054.
(20) Wilcoxen, J. P.; Newcomer, P. P.; Samara, G. A. *Solid State Commun.* **1996,** *98*, 581.
(21) Wadia, C.; Wu, Y.; Gul, S.; Volkman, S. K.; Guo, J.; Alivisatos, A. P. *Chem. Mater.* **2009,** *21*, 2568.
(22) Lin, Y.-Y.; Wang, D.-Y.; Yen, H.-C.; Chen, H.-L.; Chen, C.-C.; Chen, C.-M.; Tang, C.-Y.; Chen, C.-W. *Nanotechnology* **2009,** *20*, No. 405207.
(23) Ennaoui, A.; Schroetter, S.; Fiechter, S.; Tributsch, H. *J. Mater. Sci. Lett.* **1992,** *11*, 1131–1133.
(24) Bulatovic, S. M. *Handbook of Flotation Reagents: Chemistry, Theory and Practice, Volume 1: Flotation of Sulfide Ores*; Elsevier: Amsterdam, 2007.